Spring 2023

# Induced Drag Laboratory Curriculum with Variable Aspect Ratio Wing

Alexander Milligan
apm88@uakron.edu

Elizabeth Plyler
ejp65@uakron.edu

# Induced Drag Laboratory Curriculum with Variable Aspect Ratio Wing


By:

Alexander Milligan

Elizabeth Plyler

Project Sponsor: Dr. Nicholas Garafolo

Honors Advisor: Dr. Nicholas Garafolo

Honors Reader 1: Dr. Manigandan Kannan

Honors Reader 2: Dr. Scott Sawyer

# Abstract

A laboratory curriculum for undergraduate students at The University of Akron enrolled in 4600:413 Introduction to Aerodynamics was created to allow students a hands-on opportunity to study the basic fundamentals of aerodynamically induced drag. To accomplish this, a 3D printed wing was created with variable aspect ratio. This wing is to be utilized in the laboratory experiment in The University of Akron subsonic wind tunnel to generate data on lift on drag at different airspeeds, angles of attack, and aspect ratios. The laboratory curriculum provides basic theory applicable to the wind tunnel experiments as well as question prompts and data analysis to help students understand the impact of aerodynamic principles such as airspeed, angle of attack, and aspect ratio. Finally, students are also given the chance to design their own winglet to attach to the wing so that they may observe how their design will change aerodynamic lift and drag.

# Table of Contents

**1. Introduction....4**
1.1 Effect of Aspect Ratio on Aerodynamic Drag....4
1.2 Effect of Wingtip Vortices on Aerodynamic Drag....6
1.3 Proposed Solution....8
**2. Design....9**
2.1 Carbon Fiber Spar....9
2.2 Interlocking Mechanism....10
2.3 Wing Base to Sting Attachment....12
**3 Manufacturing....14**
3.1 Additive Manufacturing Tolerance and Test Prints....14
3.2 Assembly....14
**4 Design Verification....17**
4.1 Wind Tunnel Testing....17
**5 Laboratory Curriculum....19**
5.1 Curriculum Introduction and Theory....19
5.2 Curriculum Procedure....19
5.3 Curriculum Results....20
5.4 Curriculum Questions/Data Analysis....21
**6 Costing....22**
6.1 Labor....22
6.2 Components....22
**7 Conclusion....23**
7.1 Future Improvements....23
**References....24**

# List of Figures

Figure 1: Depiction of the generation of wingtip vortices [4]..... 6
Figure 2: Downwash flow angle [4]..... 7
Figure 3: Lift slope of finite and infinite wing [3]..... 7
Figure 4: Effect of aspect ratio on a drag polar plot [3]..... 8
Figure 5: Cross section view of spar through hole cuts..... 10
Figure 6: Wing lock peg (left) and wing lock anchor (right)..... 11
Figure 7: Exploded view of wing lock fastening mechanism..... 11
Figure 8: Wing base with trantorque insert..... 12
Figure 9: Trantorque and bronze bushing interface..... 13
Figure 10: Hole and shaft tolerance testing prints..... 14
Figure 11: Wing lock anchor piece fastened to wing..... 15
Figure 12: Wing lock peg fastened to wing..... 15
Figure 13: Trantorque inserted into fastened bushing..... 16
Figure 14: Lift slope..... 17
Figure 15: Coefficient of drag vs angle of attack..... 18
Figure 16: Drag polar..... 18
Figure 17: Demonstration winglet developed for use in the laboratory experiment..... 20

# List of Tables

Table 1: Wingspan Configurations..... 10
Table 2: Total Part Costing..... 22

# 1. Introduction

In order to be able to develop a laboratory curriculum allowing students to study the aerodynamics of lift and drag, a model wing must be designed that can allow for the study of how lift and drag changes. To understand how to design such a wing, basic principles of lift and drag must be explored. These principles will be what drives the design of the wing. In addition to the wing design, it is important to understand the aerodynamics of lift and drag to also understand the importance of aspect ratio and its effect on induced drag and overall drag.

# 1.1 Effect of Aspect Ratio on Aerodynamic Drag

Aspect ratio is an important parameter in analysis of aerodynamic forces on a wing body. To understand the importance of aspect ratio, coefficients of drag must be considered:

$$C_D = C_{D_0} + C_{D_i} \tag{1}$$

Where:

$C_D$= Coefficient drag, $C_{D_0}$= Coefficient of zero lift drag,

$C_{D_i}$= Coefficient of induced drag

Zero lift drag is dependent on airfoil geometry as well as what material the airfoil skin is made of. Parasitic drag is a component of zero lift drag and is generated due to friction forces opposing the airflow over the airfoil. This parasitic drag will increase with higher flow speeds and higher airfoil surface area.

Pressure drag is another component of zero lift drag and is generated by the airfoil wake which is the area downstream the airfoil created by flow separation. Laminar flow over the airfoil will heavily reduce the parasitic friction drag but will tend to separate from the airfoil sooner than turbulent flow, thus generating a larger wake and more pressure drag. On the other hand, turbulent flow over an airfoil will heavily increase the parasitic friction drag but will also shrink the size of the laminar boundary layer and thus delay flow separation which reduces pressure drag.

Induced drag is the other contributing factor to total drag and is the tradeoff for airfoil lifting force. Further expanding on the coefficient of induced drag:

$$C_{D_i} = \frac{C_L^2}{\pi e AR} \tag{2}$$

Where:

$C_{D_i}$ = Coefficient of induced drag, $C_L$ = Coefficient of lift,

e = Oswald efficiency factor, AR = Aspect ratio

To be able to obtain the coefficient of lift, first the lift of the airfoil needs to be measured. By using the wind tunnel force sensors, fluid velocity, fluid density, and airfoil planform area, the coefficient of lift is calculated by:

$$C_L = \frac{L}{\frac{1}{2}\rho_\infty V_\infty^2 s} \tag{3}$$

Where:

L = Lift force ($\frac{N}{m^2}$), $\rho_\infty$ = Free stream fluid density ($\frac{kg}{m^3}$),

$V_\infty$ = Free stream fluid flow velocity ($\frac{m}{s}$), s = Planform area ($m^2$)

For the purpose of this design project, the coefficient of lift and oswald efficiency factor are considered as variables and will be calculated during the laboratory experiment. However, aspect ratio is something that may be independently changed while keeping a constant wing profile section. Aspect ratio is defined by:

$$AR = \frac{b^2}{s} \tag{4}$$

Where:

b = wingspan, s = planform area

# 1.2 Effect of Wingtip Vortices on Aerodynamic Drag

Wingtip vortices are created due to the presence of a wing with finite span, and they add to the overall impact of induced drag. Equation 2 shows that a wing with infinite span will also have infinite aspect ratio and thus no induced drag. Wingtip vortices are generated due to the pressure differences required to generate lift. When the high pressure (lower wing) and low pressure (upper wing) air come in contact with each other at the wingtips, the high pressure air will force itself into the low pressure air section which generates vorticity in the fluid flow:

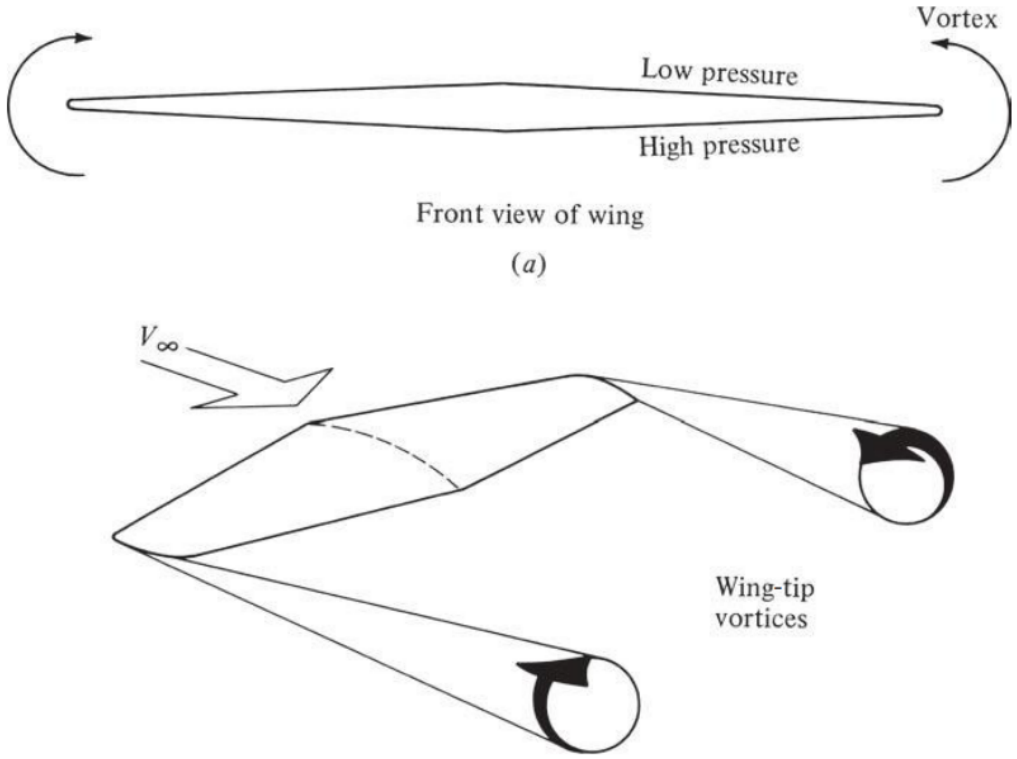


Figure 1: Depiction of the generation of wingtip vortices [4]

These vortices are not contributing to lift - they detract from the lift force. The stronger the pressure difference between the upper and lower surface of the wing, the higher the induced drag becomes. The rotational kinetic energy contained in the vortices must be overcome by increasing the aircraft propulsive system power. These vortices also contribute to downwash, which is a downward component of flow velocity downstream the airfoil. When vectorially combined with free stream velocity, the relative velocity is acting at the *effective angle of attack*,

which is the geometric angle of attack minus the downwash flow deflection angle. A depiction of this phenomenon can be seen below:

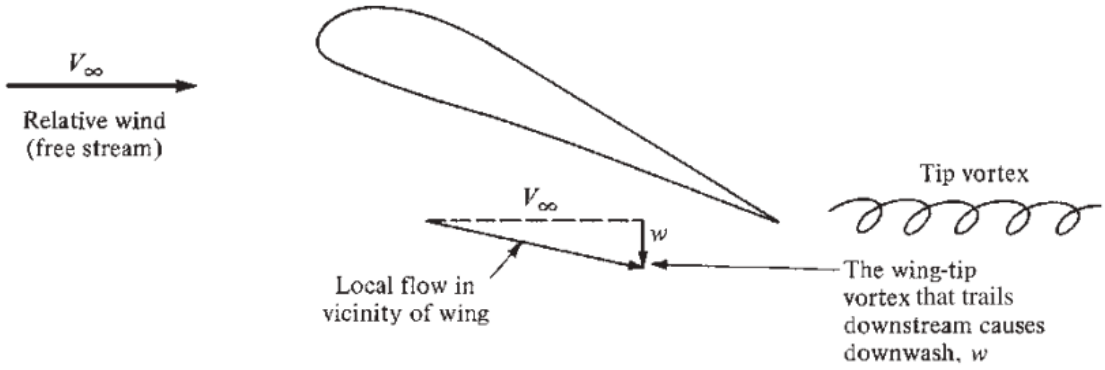


Figure 2: Downwash flow angle [4]

This effective angle of attack may also be visualized by a lift slope comparison between a finite and infinite wing. The different lift slopes show how a finite wing must operate at a greater geometric angle of attack to generate the same coefficient of lift as opposed to an infinite wing:

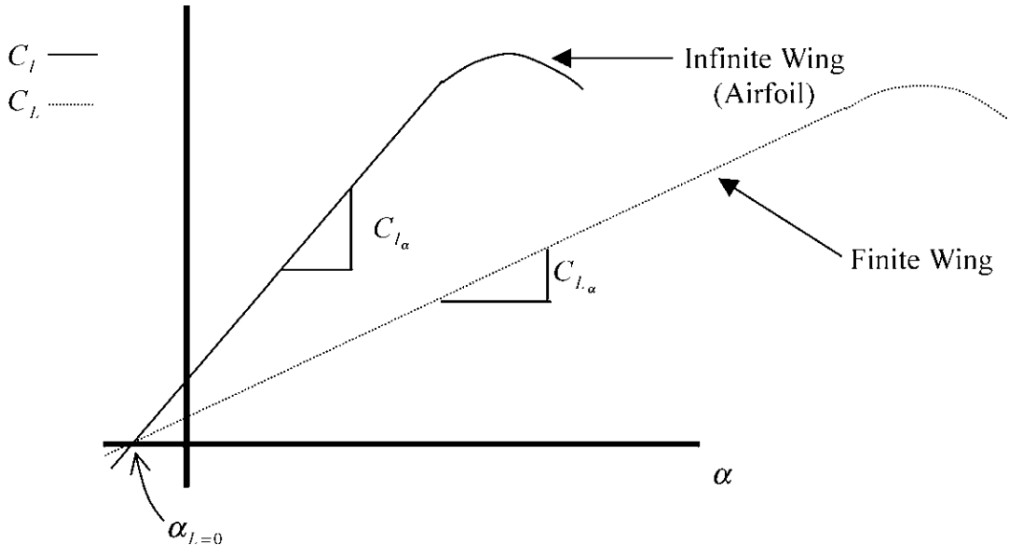


Figure 3: Lift slope of finite and infinite wing [3]

Since induced drag is proportional to the coefficient of lift squared as can be seen in equation 2, the induced drag will then exponentially increase with angle of attack as can be seen on a typical drag polar:

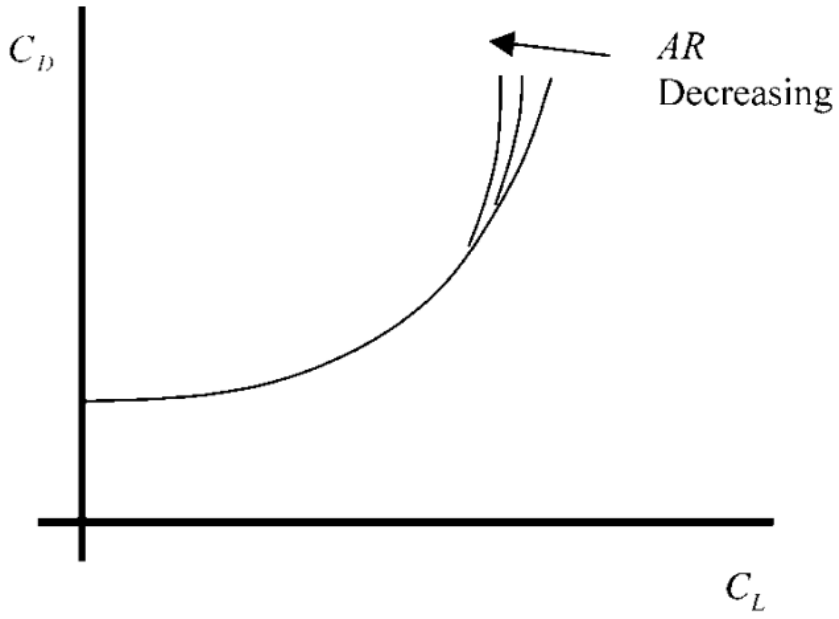


Figure 4: Effect of aspect ratio on a drag polar plot [3]

This plot also shows that with decreasing aspect ratio, the coefficient of lift will decrease at the same values of coefficient of drag. This graph will be recreated by utilizing data taken from the laboratory experiment.

# 1.3 Proposed Solution

Knowing that induced drag is a function of aspect ratio, the wing designed for use in this project will have a variable aspect ratio. Aspect ratio can be changed by the chord length of the wing and/or the span of the wing. To keep wing sections consistent, the cross sectional profile of the wing will be held constant. In other words, the chord length of the wing will remain unchanged. The aspect ratio of this design will then change by increasing and decreasing the span. To do this, a method to interlock separate wing pieces together had to be configured. This interlocking mechanism will utilize plastic peg and hole type pieces that fasten together without the use of hardware. This will allow the wing to have its aspect ratio changed quickly and easily.

# 2. Design

The design of the wing was centered around the concept of varying aspect ratio while keeping the chord line constant. This means the wing design will have a rectangular planform area with a variable span. By keeping the chord constant, the lift and drag values provided by the wind tunnel will then be a function of only wingspan and angle of attack at a given airspeed. In terms of manufacturability, it is also beneficial to fix the chord length. The thickness of the wing is a function of chord length, so by fixing the chord length, the wing thickness is also being fixed for all spans. This allows for the use of a single, uniform-diameter wing spar.

The NACA 2412 airfoil [1] was chosen for the wing profile due to its low coefficient of zero lift drag values and because it is thick enough to accommodate a half inch diameter cut that can house spars and interlocking mechanism pieces. Additionally, there is an abundance of published data available for this airfoil profile that students will be able to compare their experimental results to.

Ideally, the chord length of the wing should be as short as possible. The wind tunnel has limited width, meaning that the maximum possible span the wing could be will be fixed. With this in mind, the shortest chord length will then translate to the largest change of aspect ratio from shortest span to longest span. A method in which the wingspan could be easily changed also had to be developed by the use of interlocking wing section pieces. Interlocking these wing sections must be non-permanent and ideally require no tooling.

## 2.1 Carbon Fiber Spar

A wing model with varying aspect ratio will also experience varying lift and drag forces. To accommodate these forces, a wing spar was required. At longer spans, the wing would start to flex and this could jeopardize the data collected for use in the laboratory. To help control this wing bending, a hollow carbon fiber tube was chosen to act as the main wing spar. A roll-wrapped layered tube was chosen as opposed to a pultruded rod due to the layered tube's bending strength. This tube was cut into five different lengths to accommodate all of the possible span configurations:

Table 1: Wingspan Configurations

| Wing section | Wing base (4 in span) | Wing piece (2 in span) | Wing piece (2 in span) | Wing piece (2 in span) | Wing piece (2 in span) | Wing end piece (2 in span) |
|---|---|---|---|---|---|---|
| Total span (in) | 4 | 8 | 12 | 16 | 20 | 24 |
| Aspect ratio | -- | 1 | 1.5 | 2 | 2.5 | 3 |

Since the lift and drag act at the wing aerodynamic center, which is at the quarter chord, this was where the spar was placed. In addition to this main spar, a smaller secondary spar was added near the trailing edge of the profile. This spar is a pultruded carbon fiber solid rod. This secondary spar is much smaller and also very flexible compared to the main spar. However, the secondary spar is not used for its bending stiffness, rather is used to ensure that each wing section has an equivalent pitch angle relative to the other wing sections. These through hole spar cutouts are shown below:

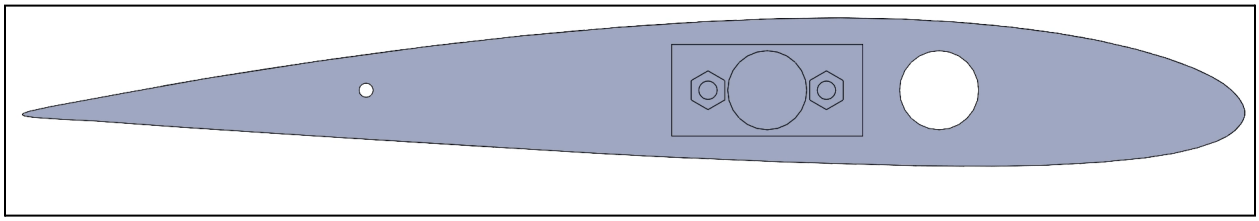

Figure 5: Cross section view of spar through hole cuts

# 2.2 Interlocking Mechanism

In order to vary the wing aspect ratio by increasing or decreasing its span, a way to interlock the different wing sections together was needed. The interlocking mechanism must be non-permanent and the wing sections must be deconstructable in order to be able to observe lift and drag at different span lengths. A few methods were considered for interlocking the wing sections together. First, an interference fit modeled after LEGO bricks with strictly 3D printed materials was attempted. This interlocking method may work with smaller tolerances, but as the tolerance of 3D printing is relatively high, this interlocking method was abandoned.

Another consideration was to use a threaded rod acting as both a wing spar and the interlocking mechanism. The wing sections would be tightened together by nuts on both ends of the threaded rod. These nuts would add considerable drag to the end pieces of the wing assembly. Due to this added drag, this interlocking mechanism was also abandoned.

In order to eliminate drag by installing fasteners to the exterior of the wing, plastic wing lock assemblies from Topmodel Model Airplane & Accessories were chosen to act as the interlocking mechanism. These wing locks operate without the use of any fasteners and are easy to assemble and disassemble. The plastic wing lock pieces are shown below as they were modeled in SolidWorks:

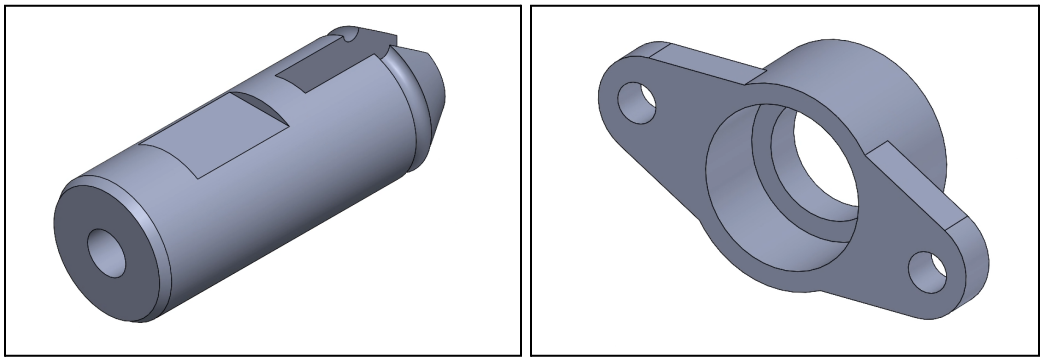

Figure 6: Wing lock peg (left) and wing lock anchor (right)

One pair of these wing locks were used per wing piece. A quarter inch space between the wing lock pieces and the spar hole was chosen to avoid any thin wall weaknesses in the 3D printed wing. The orientation of the spar and wing lock pieces in the wing sections is shown below:

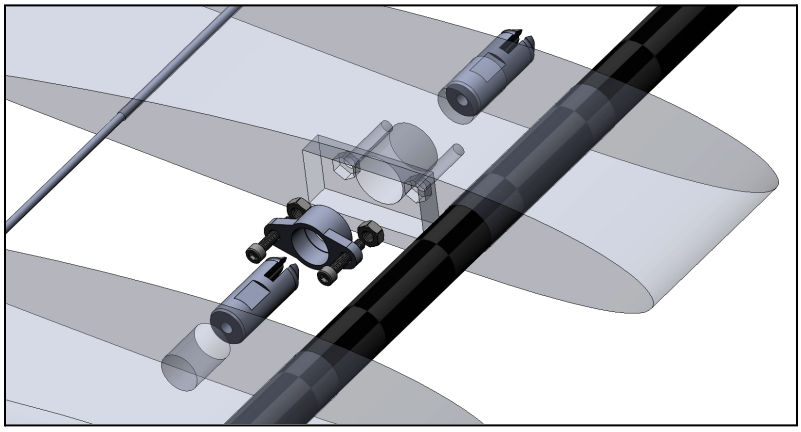

Figure 7: Exploded view of wing lock fastening mechanism

In order to fasten these wing locks to the plastic, a set of embedded M3 nuts were inserted into the plastic that allowed for the use of bolts to secure the wing lock. As for the peg-like locking piece, Cyanoacrylate super glue was used as the fastening mechanism. In order to reduce any unwanted external drag on the outboard most wing piece, this specific wing piece was designed to only have cut features on the inboard side. By designing the wing piece this way, it may be attached to the wing body at any span length making lift and drag measurements more uniform for all span lengths.

## 2.3 Wing Base to Sting Attachment

To be able to attach the wing to the wind tunnel sting, a trantorque mini interface is used. This trantorque functions as a set of nested collets where one set constricts onto the wind tunnel sting while at the same time the other set expands outward to create a friction fit between the trantorque and the wing base. This friction is created due to the radial force of the trantorque being applied to the wing base. Due to concerns of the 3D printed material fatiguing under this radial load, a bronze bushing was incorporated into the design to provide more strength to the interface between the wing base and the trantorque. This bronze bushing sits inside the housing that will also seat the trantorque. The wing base showing the bushing and trantorque mount is shown below:

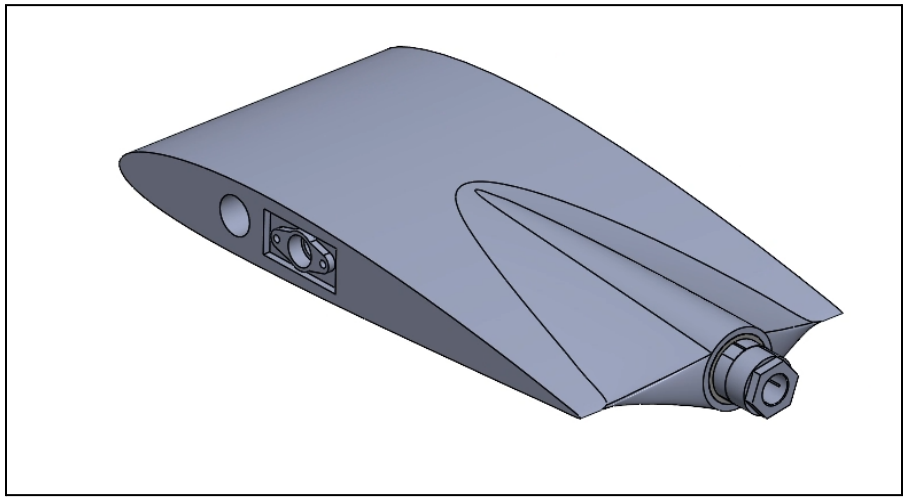

Figure 8: Wing base with trantorque insert

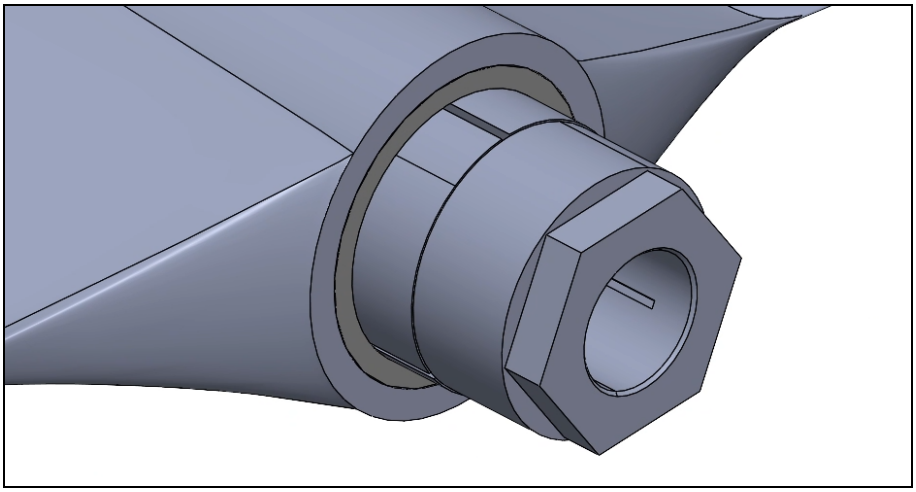

Figure 9: Trantorque and bronze bushing interface

A wall thickness of a tenth inch was chosen for the plastic seating around the bushing and trantorque mount. The bushing sits flush three quarters of an inch inside of the wing base. Since the change of induced drag is the main scope of this laboratory, the profile drag of the wing base is not a large concern. No matter the span, the wing body will always experience the same value of profile drag from the wing base. Then, if the induced drag is not changing, neither will the total drag. Knowing this, a rather large fillet was applied to the trantorque mounting area to ensure uniform stress distribution along the entire wing profile.

# 3 Manufacturing

## 3.1 Additive Manufacturing Tolerance and Test Prints

The decision to 3D print the wing sections was based on its relatively low cost and ease of redesign. In the initial phases of the project, test prints were developed that served a purpose of understanding the printing tolerances and how to stack them in a way to allow for tightly fitting components like the spars and wing locks. These test prints were carried out based on the LEGO interference fit design and can be seen below:

Figure 10: Hole and shaft tolerance testing prints

By being able to see how these hole and shaft tolerances feel, appropriate tolerances were to be decided for the final print sections. Most of the tolerances used in the design were around 0.15 in. With this tolerance, the spars are able to slide into the wing sections easily without them being loose enough yield a pitch angle instability.

## 3.2 Assembly

Once all wing sections were finished printing, assembly of the wing lock mechanism began. The anchor wing lock pieces were fastened first. To do this, M3 nuts were glued into the

plastic via an embedded cut. The plastic wing lock piece was then screwed into the nut. This assembly is shown below:

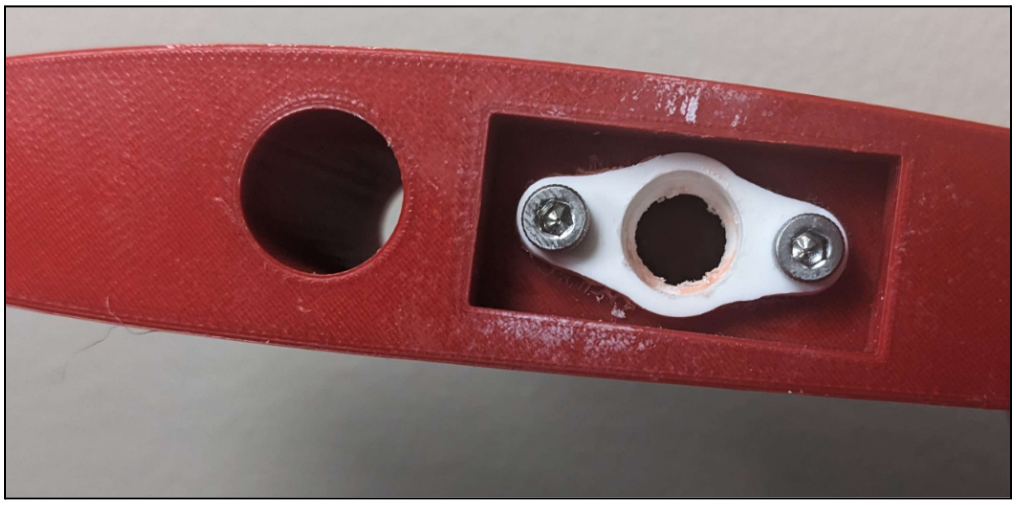

Figure 11: Wing lock anchor piece fastened to wing

Once all of these anchor pieces were secured, the peg plastic connectors had to be glued in as well. To ensure that the pegs are glued in an appropriate distance into the plastic, the pegs were first inserted into the plastic anchor piece. Then, glue was inserted into the cavity of the wing so that when the wing slides together and the glue dries, the wing may be pulled apart to disassemble the wing lock assembly. The peg can be seen glued into the wing below:

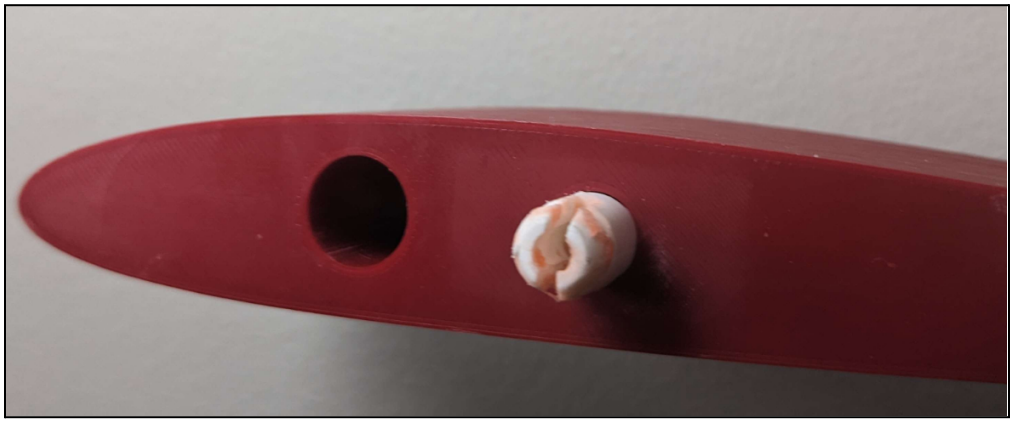

Figure 12: Wing lock peg fastened to wing

This process was completed for all 10 wing pieces (5 left pieces and 5 right pieces) as well as the wing base. Finally, the bronze bushing was glued into the wing base where the trantorque sits. The trantorque can be seen placed inside the bushing below:

Figure 13: Trantorque inserted into fastened bushing

# 4 Design Verification

After all glue was set, the wing was now able to be assembled and disassembled easily to change its aspect ratio. As for specific wind tunnel testing, students will be able to choose their specific angles of attack and airspeeds to gather data.

# 4.1 Wind Tunnel Testing

Wind tunnel testing of the wing was performed at an airspeed of 30,40, and 50 mph. At this airspeed, an angle of attack sweep from -12 to 12 degrees was performed in increments of 3 degrees. Five aspect ratios were analyzed at these conditions. Pictured below are the results of wind tunnel testing including a lift slope, coefficient of drag vs angle of attack, and drag polar at an airspeed of 50 mph:

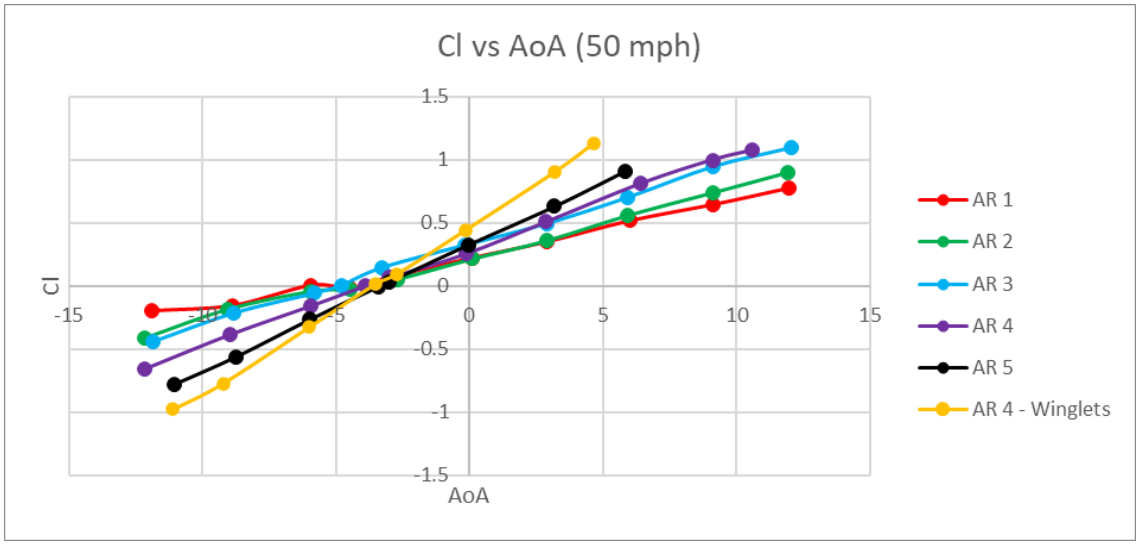


Figure 14: Lift slope

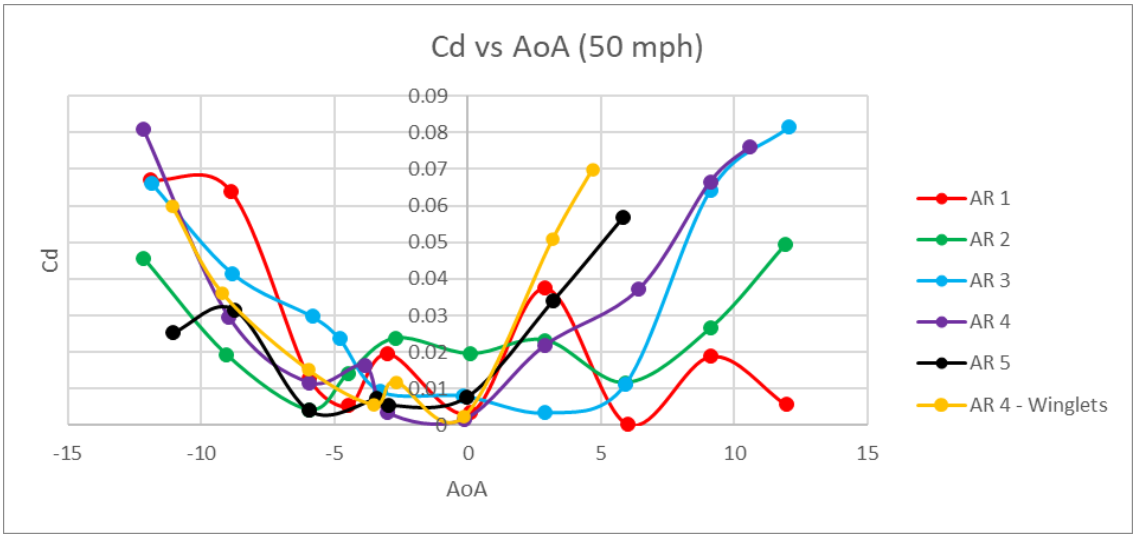


Figure 15: Coefficient of drag vs angle of attack

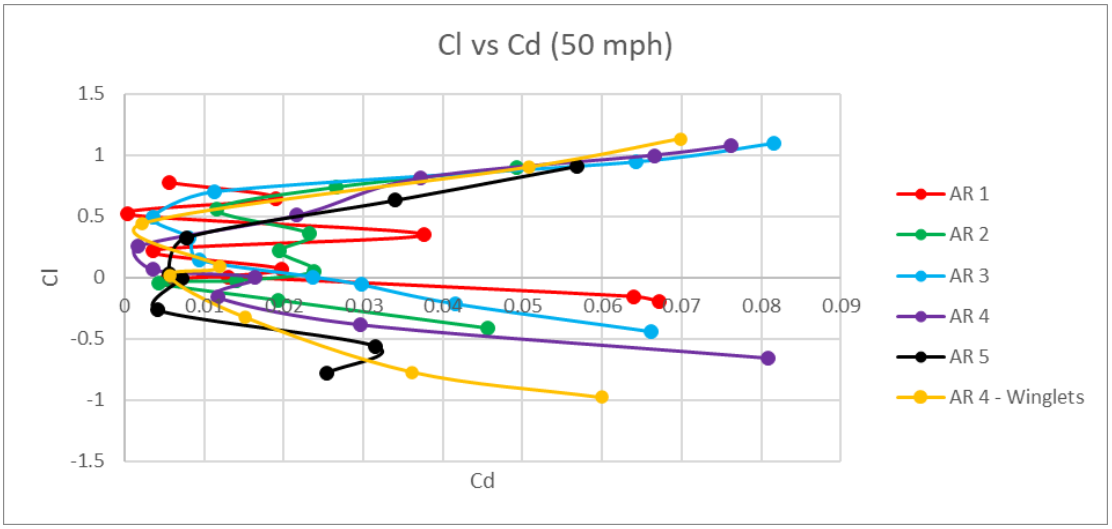


Figure 16: Drag polar

As can be seen from the lift slopes, the higher aspect ratio configuration does have a steeper slope, which is consistent with theoretical data. As aspect ratio increases, the lift slope should also be expected to increase. A wing with an infinite aspect ratio will then have the highest lift slope. The drag polar shows that the increase in aspect ratio provides more lift at the same drag values. In the future, students participating in this laboratory experiment may evaluate the wing at different airspeeds, angles of attack, and aspect ratios to discover these concepts themselves.

# 5 Laboratory Curriculum

In addition to the design of 3D printed wings with variable aspect ratio, a laboratory curriculum has been developed that will serve as an open ended guideline for students to use to learn about induced drag. The following sections will outline the curriculum's structure.

## 5.1 Curriculum Introduction and Theory

Before beginning the experiment, a section detailing information on lift and drag will be provided. In addition, a discussion around aspect ratio and wingtip vortex generation will be outlined to understand their effect on total wing drag. The majority of information presented in this section of the curriculum will be taken from the introduction of this report.

## 5.2 Curriculum Procedure

The first step in beginning the experiment will be to select airspeeds and angles of attack to evaluate the wing at. This choice will be left to the students to determine what they believe will be most appropriate. However, the curriculum acts as a guide by detailing the wind tunnel force and moment constraints.

Once airspeeds and angles of attack are chosen, students will be instructed to take measurements at each aspect ratio of the wing. They will be instructed to start at the lowest airspeed in order to avoid damaging the wind tunnel sting.

At the end of the experiment, the students will be able to utilize their custom winglet design. They will develop these winglets by editing a given CAD model with set holes set for spars and wing lock connectors. A sample winglet has been designed for use in the laboratory and is pictured below. It was inspired by modern blended winglets featured on aircraft such as the Boeing 737 and Airbus A320:

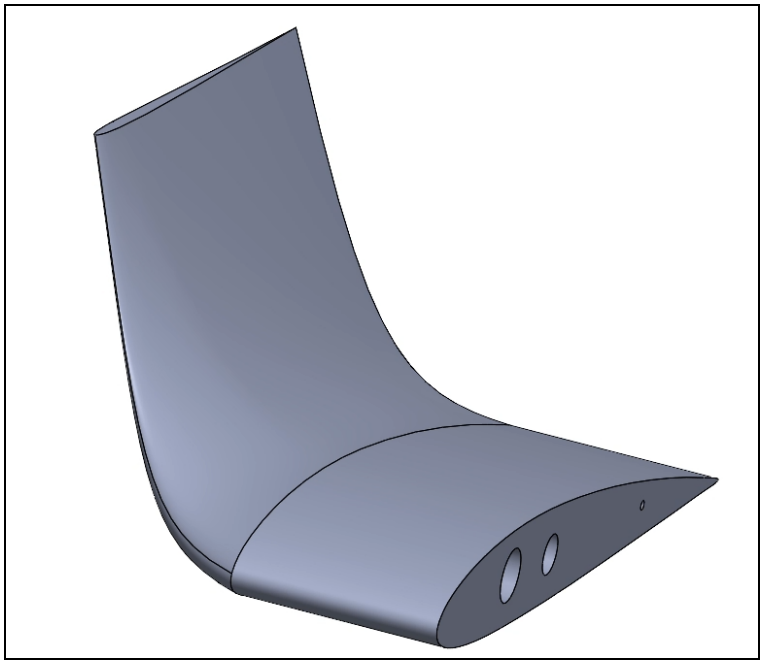

Figure 17: Demonstration winglet developed for use in the laboratory experiment

## 5.3 Curriculum Results

The results section of the curriculum will be based on the measurements of lift and drag values taken during the experiment. A summary of what will be expected of students is shown below:

- Calculate the coefficient of lift and drag from measured wind tunnel data
- Calculate the induced drag and Oswald efficiency factor at each aspect ratio, airspeed, and angle of attack configuration
- Create a drag polar, lift slope, and drag vs angle of attack plot
- Create aspect ratio vs total, zero lift, and induced drag plots

These results are easily compared to available data. The NACA 2412 is an airfoil that has been used for many decades so there is an abundance of test data for this specific airfoil shape.

## 5.4 Curriculum Questions/Data Analysis

Now that the data has been collected and processed into graphical representations, students will be asked questions to demonstrate what they have learned through the lab. These questions will ask students to explain how and why changing aspect ratio changes the total drag a

wing will experience. In addition, students will be asked to compare their calculated values of Oswald efficiency factor, coefficient of lift, and coefficient of drag to published data.

# 6 Costing

## 6.1 Labor

According to the United States Bureau of Labor Statistics, the median pay of an Aerospace Engineer was $122,270 or $58.71 per hour in May 2021 [2]. Estimating that both group members were to work an average of 5 hours total per week with a project duration of 30 weeks, the total cost in labor would add up to $8,807.

## 6.2 Components

Many different types of tools and components were used to complete this project. Shipping costs for these components were not included in the total cost of the project. A table summarizing the cost of the project can be seen below:

Table 2: Total Part Costing

| Component (Quantity) | Total Cost ($) |
|---|---|
| Bronze bushing (1) | 2.13 |
| CA glue (1) | 18.68 |
| Thick carbon fiber spar (1) | 65.99 |
| Think carbon fiber spar (2) | 25.98 |
| Trantorque mini (1) | 55.03 |
| 1kg PLA plastic spool (2) | 49.98 |
| Plastic wing lock connectors (10) | 58.40 |
| Total | 276.19 |

# 7 Conclusion

The design of a wing with variable aspect ratio has been accomplished by the use of 3D printed materials. By changing aspect ratio, drag can be studied in a real time environment at The University of Akron subsonic wind tunnel. In addition to this variable aspect ratio wing, a laboratory curriculum has been written to aid in the learning process for students enrolled in the Introduction to Aerodynamics course at The University of Akron. This laboratory curriculum outlines the basics of aerodynamic drag and allows students the opportunity to choose custom test parameters as well as testing custom winglet designs.

## 7.1 Future Improvements

Since the wing sections are 3D printed, they are inherently warped around the edges. This is an almost unavoidable artifact of 3D printing but alternative solutions to printing the wing could be considered to avoid the warping of the plastic. Printing the wing pieces in a heated enclosure would potentially help reduce warping. This warping should not drastically affect the induced drag the wing experiences due to the extra drag from plastic warping being factored out in zero lift drag.

Another aspect that may be improved upon in this design is to potentially use a thicker airfoil so that the spar and plastic wing lock connectors can still be fit in the wing profile while being able to shorten the cord length. By shortening the chord length, a greater change in aspect ratio may be achieved since aspect ratio is inversely proportional to chord length for a rectangular wing.

# References


[1] *NACA 2412 (NACA2412-IL)*, http://airfoiltools.com/airfoil/details?airfoil=naca2412-il.

[2] "Aerospace Engineers : Occupational Outlook Handbook." *U.S. Bureau of Labor Statistics*, https://www.bls.gov/ooh/architecture-and-engineering/aerospace-engineers.htm.

[3] Yechout, Thomas R. "Chapter 1: A Review of Basic Aerodynamics." Introduction to Aircraft Flight Mechanics: Performance, Static Stability, Dynamic Stability, Classical Feedback Control, and State-Space Foundations, American Inst. of Aeronautics and Astronautics, Reston, VA, 2014.

[4] Anderson, John D. "Chapter 5: Airfoils, Wings, and Other Aerodynamic Shapes." Introduction to Flight Third Edition, McGraw-Hill, 1989.